Naval Ocean Systems Center
San Diego, CA 92152-5000

Technical Report 1312
September 1989

Effects of Strong Scattering on Transionospheric Propagation

Richard A. Sprague

NAVAL OCEAN SYSTEMS CENTER

San Diego, California 92152-5000

E. G. SCHWEIZER, CAPT, USN
Commander

R. M. HILLYER
Technical Director

ADMINISTRATIVE INFORMATION

The work discussed in this report was performed by Code 542 of the Naval Ocean Systems Center.

Released by
J. A. Ferguson, Head
Ionospheric Branch

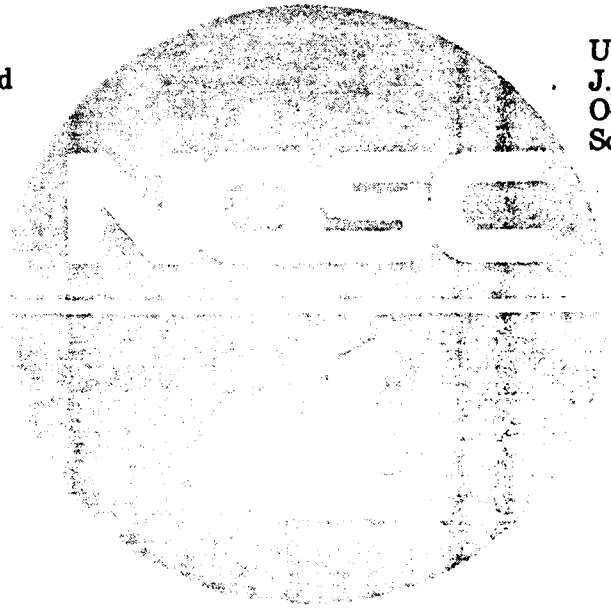

Under authority of
J. H. Richter, Head
Ocean and Atmospheric
Sciences Division

REPORT DOCUMENTATION PAGE

Form Approved
OMB No. 0704-0188

1. AGENCY USE ONLY *(Leave blank)*	2. REPORT DATE	3. REPORT TYPE AND DATES COVERED
	September 1989	Final: Oct 1987 – Sep 1988

4. TITLE AND SUBTITLE

EFFECTS OF STRONG SCATTERING ON TRANSIONOSPHERIC PROPAGATION

5. FUNDING NUMBERS

PE: 61013N
PROJ: GD30
WU: SY49

6. AUTHOR(S)

Richard A. Sprague

7. PERFORMING ORGANIZATION NAME(S) AND ADDRESS(ES)

Naval Ocean Systems Center
San Diego, CA 92152-5000

8. PERFORMING ORGANIZATION REPORT NUMBER

NOSC TR 1312

9. SPONSORING/MONITORING AGENCY NAME(S) AND ADDRESS(ES)

Naval Engineering Logistics Office
Washington, D.C.

10. SPONSORING/MONITORING AGENCY REPORT NUMBER

11. SUPPLEMENTARY NOTES

12a. DISTRIBUTION/AVAILABILITY STATEMENT

Approved for public release; distribution is unlimited.

12b. DISTRIBUTION CODE

13. ABSTRACT *(Maximum 200 words)*

This report presents preliminary results of an effort to model the effects of ionospheric electron density irregularities on transionospheric propagation. The focus of the report is on propagation at HF and low VHF, where strong multiple scattering is often encountered. A strong scattering model is therefore used to predict the effects on such parameters as the phase autocorrelation function, the spectrum of intensity fluctuations, and the fluctuation in angle of arrival. Requirements for improvements in the model and directions for later work are discussed.

14. SUBJECT TERMS

ionospheric propagation,
strong scattering,

15. NUMBER OF PAGES

41

16. PRICE CODE

17. SECURITY CLASSIFICATION OF REPORT	18. SECURITY CLASSIFICATION OF THIS PAGE	19. SECURITY CLASSIFICATION OF ABSTRACT	20. LIMITATION OF ABSTRACT
UNCLASSIFIED	UNCLASSIFIED	UNCLASSIFIED	

CONTENTS

PREFACE v

INTRODUCTION 1

F-REGION ELECTRON DENSITY IRREGULARITIES 2

Amplitude Characteristics 3

Spectral Properties of Irregularities 4

EFFECT OF ELECTRON DENSITY IRREGULARITIES ON TRANSIONOSPHERIC PROPAGATION 8

MULTIPLE REFRACTIVE SCATTER MODEL 9

IMPLEMENTATION OF THE MULTIPLE REFRACTIVE SCATTER MODEL 22

SUMMARY 29

REFERENCES 30

PREFACE

This report presents the results of modeling the effects of electron density irregularities on transionospheric propagation. The objective of this effort has been to provide a tool for determining, in real time, the expected effects of such irregularities on the performance of a given transionospheric monitoring system. While these effects can take several forms, we concentrate here on the variation in the phase of the signal due to scattering caused by such irregularities.

In this report, we shall be mainly interested in remote locating systems. Such systems rely on accurate measurements of the phase difference between separated receive antennas to provide estimates of apparent angular location (azimuth/elevation). Fluctuations in this phase difference due to scattering caused by electron density irregularities result in a consequent fluctuation in the apparent location of the transmitter. System performance can be seriously degraded if the correlation in the phase fluctuation between antennas is low or the mean square fluctuation in phase is large. In any case, the accurate determination of the phase fluctuations provides an estimate of the error for a given location estimate and thus provides important information for the system user.

Another feature that must be addressed under strong multiple-scattering conditions is the reduction of correlation in the intensity of the signal. Under such scattering conditions, defocusing by large scale* irregularities can cause deep small-period fades in signal strength. For sufficiently strong scattering, these signal fades may have a spatial extent on the order of the size of the locating system (tens of meters). This loss of signal makes the system unreliable at best and, in some cases, inoperable.

This area of investigation is not completely new; there exists a large body of related work. What is different about this effort is the extension to low VHF and HF operational frequencies. Previous work has, for the most part, dealt with higher frequencies where, in general, the relatively simple single-scatter models are applicable. Also, at these frequencies, one can generally ignore the refractive effects of the background ionization. This simplifies the implementation of the models considerably.

At lower frequencies, strong multiple refractive scattering by large scale irregularities becomes the rule rather than the exception. Also, refractive effects of the background ionosphere become extremely important and must be included for accurate modeling. Thus applicable models become much more complicated and their use in a real-time situation doubtful. However over the last decade or so, Professor H.G. Booker of the University of California at San Diego has developed a model suitable in these situations. This model is described and used in this report to provide a means of calculating the effects described above.

*In this report the term "scale" will always refer to wavelength (λ) divided by 2π.

INTRODUCTION

In this report, we consider the propagation of electromagnetic waves within a bounded plasma medium. If the characteristics of such waves are known before their penetration into such a region, measuring the same characteristics after the waves exit is a direct means of determining the properties of the plasma medium itself. For example, the deviation of ray direction for a pulse of suitable carrier frequency after traversing the earth's ionosphere provides a means of determining the magnitude of electron density gradients within the ionosphere.

Another example is the modulation of the wavefront which often occurs when a wave traverses the ionosphere. This modulation is caused by irregularities of electron density which exist within the ionosphere. The variation in phase across the wavefront produces interference, and eventually, amplitude fluctuations at a distant receiver. One way of determing the amplitude and scale of the irregularities within the ionosphere is to measure the magnitude and scale of these amplitude fluctuations. This is the phenomenon known as amplitude scintillation and, along with the phase fluctuations, known as phase scintillation, is the subject of this report.

For transionospheric propagation, the effects of the scattering can take several forms, depending on the characteristic of the wave being measured. For transionospheric communication systems, the effects of scattering can be significant. The deep high-frequency fading of signal levels having a duration of minutes or even hours can cause extended periods for which communication may be impossible.

Scattering can also affect burst communication systems, which require coherent signals over a large bandwidth. Frequency dependence of the scattering causes significant dispersive effects, which can drastically reduce effective signal bandwidth.

Locator systems, which use multiple receiving antennas for remote detection, are also greatly affected. Such systems rely on differences in the phase of received signals at each antenna to determine the location of the transmitter. Fluctuations in the phase of the signal caused by the scattering process cause apparent variations in the location of the transmitter. Under very strong scattering conditions, the phase fluctuations can become large enough to render such locator systems incapable of operation.

Several methods are available for modeling the effects of scattering on transionospheric propagation. Methods employed differ, depending on whether the scattering is weak or strong. If the scattering is weak, which we will define more rigorously later, the weak or single-scatter modeling methods are applicable. These include the Born Approximation (Ishimaru, 1978), the Rytov or smooth perturbation method (Tatarskii, 1971; Ishimaru, 1978), and the phase-changing screen method of Booker (Booker *et al.*, 1950). These methods are usually adequate at very high frequencies or under extremely quiescent ionospheric conditions.

At lower frequencies or under highly disturbed conditions, strong or multiple scattering becomes the rule. Theories which describe the scattering under these conditions are generally extremely complicated and are therefore not amenable for use in an operational environment. Two of the currently popular methods of this type in use are based on the parabolic approximation to the wave equation. These are the path integral method (Dashen, 1979) and the moment method (Ishimaru, 1978).

Another much simpler method is the multiple refractive scatter model developed by Booker (Booker, MajidiAhi, 1981). In this method, the multiple-scattering region is replaced by a single "deeply modulated" phase-changing screen. This amounts to replacing

a multiple small-angle scatter situation with a single "large" angle one. At first glance, the validity of such an approximation is questionable. However, it has been shown (Booker *et al.*, 1985) that as long as the centrally located phase screen (1) has effective irregularity sizes perpendicular to an incident ray which are identical to those in the medium, and (2) produces the same total mean-square value of phase fluctuations as the actual medium, the theory produces results substantially the same as the more elaborate theories mentioned above. The relative simplicity of the multiple refractive scatter model also makes it attractive for use in an operational environment. For these reasons, this model was chosen for this project and is the model described in this report.

Any model used to predict the effects of F-region electron density irregularities on transionospheric propagation requires an accurate description of the properties of the irregularities themselves. Fortunately, a large literature exists detailing the results of experiments designed to measure these properties. In the next section, we give a general overview of the findings.

F-REGION ELECTRON DENSITY IRREGULARITIES

A great deal of research has been done on the mechanisms which produce electron density irregularities in the ionosphere. Generally speaking, it has been found that the experimentally determined properties of the irregularities are consistent with various plasma wave instability processes. These processes differ on a global scale, so that the mechanism thought to produce equatorial "bubble" irregularities, for example, is different from that which is supposed to produce auroral "blob" irregularities. This variability of causative mechanisms makes difficult the development of a unified global picture of the generation of electron density irregularities.

A discussion of the processes for the generation of ionospheric irregularities is outside the scope of this report. Readers interested in further information are directed to Fejer, Kelley, 1980; Heelis, 1987; and Tsunoda, 1988. In this report, we simply assume the existence of the irregularities in the F-region ionosphere and attempt to describe their general physical properties. Later we will relate these properties to the observed properties of the scattering phenomena they produce.

Ground-based scintillation measurements are one means of probing the irregular structure of the ionosphere. Among other important measurement techniques are ground-based polarization rotation measurements (Yeh *et al.*, 1979), *in situ* measurements by rocket and orbiting satellites (Singh, Szuszczewicz, 1984; McClure, Hanson, 1973; Clark, Raitt, 1976), and radar backscatter measurements (Woodman, LaHoz, 1976). All these techniques have been used to produce a general description of the physical properties of F-region electron density irregularities for scale sizes from several meters to hundreds of kilometers.

One important characteristic of ionospheric plasma, which we will not discuss in depth in this report, is its motion with respect to the earth. This motion is caused by forces produced by various natural mechanisms, among which are neutral atmospheric winds, neutral atmospheric acoustic gravity waves, and the interaction of the earth's magnetic field with induced electric fields. These forces cause the plasma, and hence the irregularities, to drift in complicated patterns.

In all experimental systems designed to measure the spatial properties of electron density irregularities, the data are actually determined in the form of a time series. For example, a single ground-based receiver in a transionospheric scintillation experiment

measures the changes in the signal as a function of time. This temporal information is multiplied by an "effective" velocity of the irregularities to provide information about their spatial characteristics. This effective velocity is determined, in any given experiment, by any or all of the natural mechanisms listed above. Thus, it is possible to describe the properties of electron density irregularities in either temporal or spatial terms. In this report, we discuss the irregularities in spatial terms, as is customary in the literature.

The properties of the irregularities important in determining the nature of the scattering are their amplitude and their spatial power spectral density or power spectrum. The amplitude determines the strength of the interaction between the irregularities and an electromagnetic wave. The power spectrum determines the spatial extent of the interaction. We shall treat each separately below.

AMPLITUDE CHARACTERISTICS

Most of the current knowledge concerning the fluctuation amplitude, $\Delta N/N$, of electron density irregularities has been gained through the use of rockets and orbiting satellites. These *in situ* methods only produce information in one spatial dimension, the direction of travel of the platform, so a complete three-dimensional description requires the combination of results from various experiments.

Generally, the irregularity amplitudes that are observed differ between high latitudes, mid-latitudes, and equatorial latitudes. At mid-latitudes, the F-region ionosphere seems to be remarkably smooth. An analysis of data from the satellite Ogo 6 (perigee ~400 km, apogee ~1100 km, inclination ~82 degrees) by McClure and Hanson (1973) shows average root-mean-square (rms) values of amplitude of about 0.1% for irregularities with wavelengths less than 100 km. (Irregularity sizes are usually given in either wavelength or scale.) This value is also observed in nighttime when scintillation activity is usually most intense (McClure, Hanson, 1973).

A more extensive data set collected by the satellite ESRO-4 (perigee ~240 km, apogee ~1177 km, inclination ~91 degrees) was analyzed by Clark and Raitt (1976). These authors organized approximately 1.5 years of rms amplitude data into contour plots of location vs. local time. Due to the precession of the orbital plane, it was possible to order their data according to altitude. The results, valid for irregularity wavelengths between about 7 m and 7 km, show that for magnetically quiet periods ($K_p \leq 3$), average values of rms amplitude are less than or about 2%. This is for amplitude values averaged over a height range of 400-1000 km. Again, this value is for both day and night periods (Clark and Raitt, 1976).

In the restricted height range of 400-600 km (i.e., just above the F-region peak) subauroral zone structure tends to merge with mid-latitude structure at nighttime to produce average rms amplitudes as high as 4%. This structure also extends to the equatorial region where contours from the northern and southern hemispheres join. This produces the only evidence of significant equatorial irregularities (~4%) seen by Clark and Raitt (1976). Similar results were found for magnetically disturbed periods although, in this case, nighttime subauroral structure is evident (~2%) at mid- and equatorial latitudes even when averaged over the full height range of 400-1000 km (Clark, Raitt, 1976).

One phenomenon observed at all latitudes, but especially in the equatorial region, is "spread-F." The term "spread-F" is used to describe a scattering phenomenon in which F-region ionograms show echoes which are spread over a range of heights or frequencies. When a range of frequencies near the peak frequency shows returns from many height ranges, the condition is often termed "range spread-F" and is associated with strong scintillation activity (Aarons, 1982).

The spread-F phenomenon has been the subject of much research since it was first observed in the mid-30s (Booker, Wells, 1934). The equatorial occurrence of the phenomenon is thought to be caused by large scale (~100 km) bubble irregularities observed in postsunset hours. These regions of depleted electron density are believed to be generated by bottomside instability processes, where they produce the spread-F signature on ionograms (Fejer, Kelley, 1980). Once formed, the bubbles rise to heights above the F-layer peak, where they produce transionospheric scintillation effects (Fejer, Kelley, 1980). The scintillation is believed to be caused by smaller scale, large-amplitude (~100%) irregularities formed at the steep density gradients at the edges of the bubble. This phenomenon, while somewhat localized in time and space, produces the most intense scintillation observed (Aarons, 1982).

At high latitudes, the location of the auroral oval provides a scintillation boundary between mid-latitude and auroral zone irregularity structure. The analysis of Clark and Raitt (1976) shows that at all height levels from 400 to 1000 km, the equatorial boundary of the auroral scintillation region reaches a geomagnetic latitude of ~40 degrees in the nighttime sector. Within this nighttime subauroral region, these authors find that almost 60% of the time, rms values of amplitude are greater than 5%; and almost 100% of the time, they are greater than 2%. Peak values in this region reach 8%–10% at all height ranges. This behavior extends poleward of the auroral zone, with only a small decrease in observed intensity (Clark, Raitt, 1976).

In summary, the experimental data show that irregularity amplitudes differ according to location and local time. At high latitudes, the irregularities are generally of largest amplitude, especially in the region of the nighttime auroral zone. These large-amplitude irregularities continue only slightly diminished across the polar region.

At mid- and equatorial latitudes, irregularities are generally much less intense. However, at heights close to the F-region peak, nighttime subauroral zone structure tends to reach equatorward. This produces the only significant average irregularity intensities in this region.

In a more localized sense, large-amplitude irregularities are often seen in coincidence with nighttime spread-F. While spread-F can occur at any latitude, it is most often seen at equatorial latitudes, where it produces the most intense scintillation activity.

SPECTRAL PROPERTIES OF IRREGULARITIES

Electron density irregularities in the F-region ionosphere have been observed over a large range of scale sizes, from several meters to thousands of kilometers. The largest of these irregularities are associated with tidal motions and planetary scale wave motions (Livingston *et al.*, 1981), while the smallest are associated with the turbulent decay of intermediate scale structures. Between these extremes lies a scale range for which the spatial power spectrum can be characterized as power law. The irregularities responsible for the scintillation observed on the earth lie largely within this range.

The extremes of the power law scale range are determined by two particular scale sizes. At the small scale (large wave number) end, the "inner scale" is thought to lie at approximately the ion gyroradius (~3 m) (Booker, Ferguson, 1978; Woodman, Basu, 1978).

At the large scale (small wave number) end of the spectrum, there is some debate as to the location of the "outer scale." Some workers believe that no identifiable largest scale size irregularity exists. They argue that the large scale irregularities merge smoothly into nonirregular "trends," such as the diurnal effects of solar radiation, and so a separation scale between irregular and deterministic effects is impossible to define. In this case,

the largest scale size of importance in any operational situation is determined by system parameters, such as integration time or bandwidth of a receiver (Rino, 1979).

However, others argue that a definable effective outer scale does exist but has not been detected to date because of the detrending technique that has been used in analyzing measured data. The detrending procedure is commonly used to remove a deterministic component from a given data set. For example, when phase variations of the signal from an orbiting satellite are analyzed, the known effect of the satellite motion is removed in order to isolate the variation due to scattering. However, if the detrending frequency is higher than any frequency components contained in the data, all the lower frequency content is lost in this procedure. It is the low-frequency component of the data which contains the effects of the large scale irregularities, and therefore removing this component makes it impossible to identify an outer scale from phase scintillation data.

Booker argues (Booker, 1979) that the turbulence-like power law spectrum (see below) which is observed results from the cascade of energy from the large outer-scale irregularities to smaller scale sizes. The outer-scale irregularities are produced by travelling ionospheric disturbances (TIDs), which seem to be present to one degree or another at most times in the F-region ionosphere.* TIDs are produced by the interaction of neutral atmospheric acoustic gravity waves with the ionized component of the atmosphere (Hines, 1960). The amplitude of the gravity waves at any height is dependent on the scale height of the atmosphere at that height (Hines, 1960). This leads Booker to identify the outer scale of the irregularity spectrum with the neutral atmospheric scale height (Booker, 1979; Booker, Tao, 1987).

In order to resolve the question of the existence of a physical outer scale of turbulence, an experiment must be designed to determine the spectrum at low frequencies. Until then, the question remains open.

Between the inner scale and outer scale, however it may be defined, the power spectrum of irregularities is characterized by the form k^{-p}, where k is the wavenumber (1/scale size) and p is the spectral index. In general, the results from *in situ* measurements (i.e., one-dimensional) show that p ranges between 1.5 and 2.5, with values close to 2 being most common. This result is found at both high (Phelps, Sagalyn, 1976) and equatorial (Livingston *et al.*, 1981) latitudes for irregularities from ~100 m to several hundred kilometers.

Consistent with these results for the power spectrum, the spectral index for the amplitude spectrum is approximately unity (McClure, Hanson, 1973). Thus, the average amplitude $<\Delta N/N>$ is approximately proportional to scale size (McClure, Hanson, 1973). Further, the actual spatial gradients of electron density are approximately independent of scale size, depending only on the density of the ambient plasma.

Some more recent results have indicated a systematic decrease in the spectral index for strong perturbation strengths (Livingston *et al.*, 1981). Similar effects have been observed in phase scintillation data taken under strong scatter conditions (Livingston *et al.*, 1981). Thus, in some modeling situations, it may be appropriate to consider two values of the spectral index.

---

*A. Paul of NOSC, private communication, 1988.

The general spectral properties described above have been summarized by Booker (1979) and are shown in Fig. 1. This figure actually represents the inferred two-dimensional spectrum for irregularities isotropic in planes perpendicular to the earth's magnetic field. For the two-dimensional spectrum, the spectral index is $p + 1$. Also indicated in Fig. 1 is the portion of the spectrum responsible for the various scattering phenomena observed.

In situ data provide spectral information in only one spatial direction. A full three-dimensional description of the electron density irregularities requires multitechnique experiments. From intensity and phase scintillation measurements of transionospheric signals, it has been found that the electron density irregularities are structured by the earth's magnetic field. Results from the Wideband satellite, for example, confirm earlier results that the electron density irregularities are aligned along the earth's magnetic field lines (Rino, Livingston, 1982). At equatorial latitudes, the alignment is in the form of rod-like structures elongated along the magnetic field lines. Analysis of Wideband satellite data (Secan, Fremouw, 1983) shows that for irregularities up to about 20-km cross-field wavelength, the ratio of the scale size along the field to across the field is about 30:1. This ratio is reduced as the latitude increases to about 8:1 (Secan, Fremouw, 1983).

At auroral latitudes, the Wideband phase scintillation data show an increase in the mean-square fluctuation of phase when the satellite line-of-sight lies within the local L shell. This is found to occur even when the satellite is not in the same meridian as the receiving site (Rino *et al.*, 1978). This phenomenon has been interpreted as implying an elongation of the irregularities in the magnetic east–west direction within an L shell (Rino *et al.*, 1978). The observed extent of this elongation along a second axis is a more complicated function of local magnetic time and of the position of the line-of-sight ionospheric penetration point within the auroral region (Secan, Fremouw, 1983).

The results quoted above are based on ground-based measurements of the phase scintillation on signals from the Wideband satellite. These data were routinely detrended at a period of 10 seconds before analysis (Fremouw *et al.*, 1978). Thus, the results are strictly valid for irregularities with scale sizes of a few kilometers or less. Evidence indicates that large scale irregularities ($\sim$ outer scale and larger) are approximately magnetically isotropic (Booker, 1979).

In summary, the spectral properties of electron density irregularities are basically independent of global location. Results from different experimental methods all indicate a power law spectrum with a one-dimensional spectral index near 2.

Irregularities up to about 3 km are observed to be structured by the earth's magnetic field. This structure takes the form of rod-like irregularities at equatorial and mid-latitudes. At auroral zone latitudes, the rod-like structure gives way to a sheet-like structure, where elongation is within the local L shell.

In the next section, we describe the multiple refractive scatter model. This will require an analysis of the phase-changing-screen modeling technique. First, however, we provide an intuitive description of the multiple-scattering process and how it differs from weak scattering.

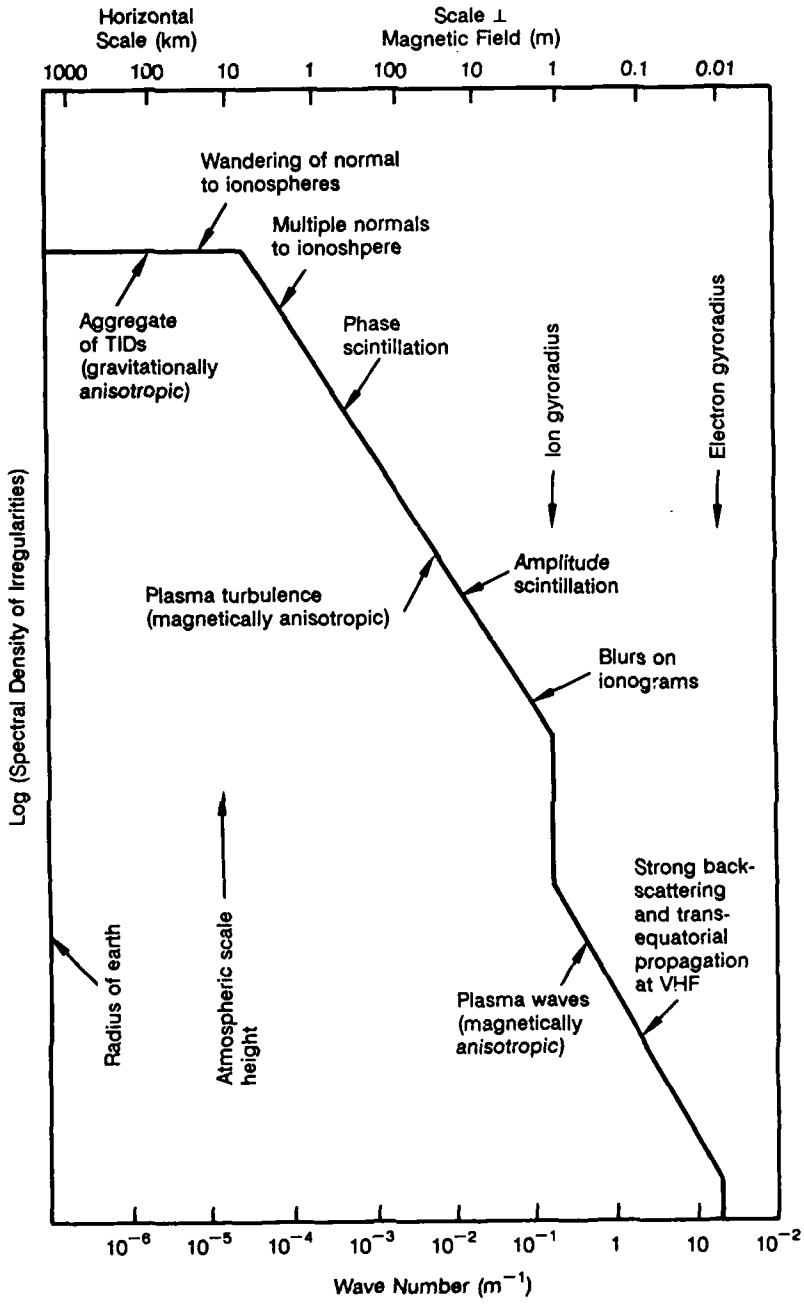

Figure 1. Representation of the power spectrum of ionospheric irregularities. Portions of the spectrum responsible for various scattering phenomena are indicated on the figure (after Booker, 1979).

EFFECT OF ELECTRON DENSITY IRREGULARITIES ON TRANSIONOSPHERIC PROPAGATION

Consider a plane electromagnetic wave of frequency f and wavelength λ incident at an arbitrary angle on an extended plasma medium. If f is larger than the peak plasma frequency, the wave will propagate into the plasma. Assume that this region contains a random distribution of electron density irregularities with sizes ranging from about $\lambda/2\pi$ to some outer scale size which is much greater than $\lambda/2\pi$. As the wavefront propagates within the medium, the variation of refractive index it encounters causes sections of the wavefront to advance with respect to the main wave and other sections to recede. This results in a random "corrugation" of the initially plane wavefront which we can describe in terms of the rms variation in phase, $<\Delta\phi^2>^{1/2}$, across the wavefront. As the wave continues to propagate, diffraction effects cause amplitude variations to develop across the wavefront. The distance the wave must travel before amplitude variations develop is dependent on $<\Delta\phi^2>^{1/2}$, λ, and the scale size of the irregularities.

Let ΔL be the depth of penetration of the wavefront within the medium. When the wavefront first enters the medium, the rms variation of phase across the wavefront is very small, and hence any resulting amplitude variations are also very small. For the ionosphere, the density irregularities one normally encounters have a small enough amplitude that even for ΔL on the order of the outer scale size of irregularities, the rms phase variations across the wavefront remain small, i.e., $<\Delta\phi^2>^{1/2}$ less than 1 radian. Here, the weak or single-scatter approximation is adequate to describe the resulting amplitude variations. The result is that a set of receivers at some distance Z measures amplitude variations of spatial size about equal to the Fresnel scale, suitably modified by the propagation geometry. The energy lost by the main wave, which goes into producing the amplitude fluctuations, is small and so also is the rms variation of the amplitude fluctuations.

As the wave continues to propagate and ΔL becomes much larger than the outer scale size of the irregularities, the wave is "scattered" many times. If the amplitude of the irregularities is large enough, this results in an rms variation of phase across the wavefront which can be much greater than unity. Here, then, it is the largest scale size irregularities which, after many scatters, produce the largest part of the phase variations. When $<\Delta\phi^2>^{1/2}$ becomes large enough, the ionosphere begins to act like an optical lens and produces focusing. Receivers at distance Z then measure amplitude variations which are smaller in spatial extent than the Fresnel scale. These small scale variations are, in fact, being produced by the large scale irregularities in the medium. The energy lost by the main wave in producing these amplitude variations is considerable, and the rms variation of the amplitude fluctuations can be very large.

From the above description, we see that the scattering one encounters for transionospheric propagation differs according to various situations. If the extent of the propagation region is small or the amplitude of the irregularities is also small, then the weak-scatter theory may be used to describe the phenomena. The result is that weak amplitude variations develop which have a characteristic size of about the Fresnel scale for the receiving location. However, if the propagation distance extends over large distances, multiple scattering of the wave can produce large variations in the rms phase. Here, it is the largest size irregularities which act to produce small scale amplitude variations at a receiver. It is this latter instance of strong or multiple scattering that we are mainly interested in in this report. In the following section, we will describe this scattering process in more quantitative detail by introducing the concept of the phase-changing screen.

MULTIPLE REFRACTIVE SCATTER MODEL

Before we can understand the multiple refractive scatter theory, we will need to describe the phase-screen modeling technique. This is done most easily by using the concept of an angular spectrum of plane waves (Booker *et al.*, 1950). Such a spectrum can be used to synthesize an arbitrary function of spatial coordinates in terms of component plane waves, just as the Fourier integral can be used to analyze a suitable temporal function in terms of its component frequencies. We will use the angular-spectrum method to determine the diffraction field produced by a sinusoidal phase-changing screen. Although this is an extreme simplification of our actual problem, it does allow the generation of results which are also valid for the more general situation to be described later.

For this section, we will follow Ratcliffe (1956) and consider plane waves normally incident on a one-dimensional phase screen. This will be generalized to a two-dimensional screen and obliquely incident spherical waves when we describe our implementation of the model.

To introduce the concept of an angular spectrum of plane waves, we consider an infinite two-dimensional screen, the X-Y plane at $Z = 0$, which is uniform in the Y direction. Let a system of uniform plane waves of frequency f and wave number k travelling in directions making angles + and $-\theta$ with the Z axis make up an angular spectrum of plane waves. We assume that the waves are polarized in the X-Z plane and that the resultant complex amplitude of those waves, with wave normals between θ and $d\theta$, is $A(\theta)d\theta$. Then the corresponding bundle of waves is given by

$$A(\theta)d\theta\, e^{ik(X \sin\theta + Z\cos\theta)}$$

where a time factor $e^{-i\omega t}$ has been omitted. The total field amplitude at a point X,Z is given by

$$\int_{-\pi/2}^{\pi/2} A(\theta)(C,0,-S)\, e^{ik(XS+ZC)}d\theta$$

where $C = \cos\theta$ and $S = \sin\theta$. In particular, the amplitude of the X component, call it $w(X,Z)$, is given by

$$w(X,Z) = \int_{-\pi/2}^{\pi/2} A(\theta)C\, e^{ik(XS+ZC)}d\theta$$

or with $d\theta = dS/C$ and $A(\theta) = W(S)$

$$w(X,Z) = \int_{-1}^{1} W(S)\, e^{ik(XS+ZC)}dS \qquad (1)$$

This represents a wave field varying over X and Z written in terms of an angular spectrum, $W(S)$, of plane waves. Over the screen at $Z = 0$ we have

$$w(X) = \int_{-1}^{1} W(S)\, e^{ikXS}dS$$

If we let $k = 2\pi/\lambda$ and measure distance in units of wavelength λ, this becomes

$$w(x) = \int_{-1}^{1} W(S)\, e^{i2\pi Sx} dS$$

where $x = X/\lambda$. For the remainder of this section, lower case letters represent distances in units of wavelength unless otherwise stated.

From these results, we see that $W(S)$ and $w(x)$ are Fourier transform pairs if we extend the integration limits to $\pm\infty$. We will do this since values of $|S| > 1$ correspond to evanescent waves which decay within several wavelengths of the screen. Consequently, at planes separated from the screen by more than a few wavelengths, only propagating fields for which $|S| < 1$ will exist. So we can write

$$w(x) = \int_{-\infty}^{\infty} W(S)\, e^{i2\pi Sx} dS \tag{2}$$

and

$$W(S) = \int_{-\infty}^{\infty} w(x)\, e^{-i2\pi Sx} dx \tag{3}$$

Likewise, Eq. 1 becomes

$$w(x,z) = \int_{-\infty}^{\infty} W(S)\, e^{i2\pi(xS+zC)}\, dS \tag{4}$$

The above analysis shows that an angular spectrum $W(S)$ will produce on the screen at $Z = 0$ a field component along X given by $w(x)$, where $w(x)$ and $W(S)$ are transform pairs. This implies that a field $w(x)$ over the screen, however it may be produced, is equivalent to the angular spectrum $W(S)$.

As a simple example, consider an angular spectrum consisting of just two plane waves making angles $\pm\theta_0$ with the Z axis and having complex amplitudes $W(S_0) = (a/2)$ exp $(i\phi)$ and $W(-S_0) = (a/2)$ exp $(-i\phi)$, where $S_0 = \sin\theta_0$. Then, from Eq. 4, the resulting field amplitude at a point x,z is

$$w(x,z) = W(S_0)\, e^{i2\pi(-S_0x+C_0z)} + W(-S_0)\, e^{i2\pi(-S_0x+C_0z)}$$

$$= a\, e^{i2\pi C_0 z} \cos(2\pi S_0 x + \phi)$$

This represents a waveform travelling along the $+Z$ direction with an amplitude which varies sinusoidally along the wavefront with wavelength D. The spatial period $d = D/\lambda$ of the sinusoidal variation is given by $2\pi S_0 = 2\pi$ or $d = 1/S_0$. In Fig. 2. we show the resulting wavefront and the corresponding angular spectrum (Ratcliffe, 1956).

The velocity in the Z direction of this striated wavefront is given by $v_0 = f/C_0$, where we recall that we are assuming sinusoidal time development and that distances are measured in units of λ. If we let $v = f$ be the velocity of a uniform plane wave and write $C_0 = (1 - 1/d^2)^{1/2}$, then

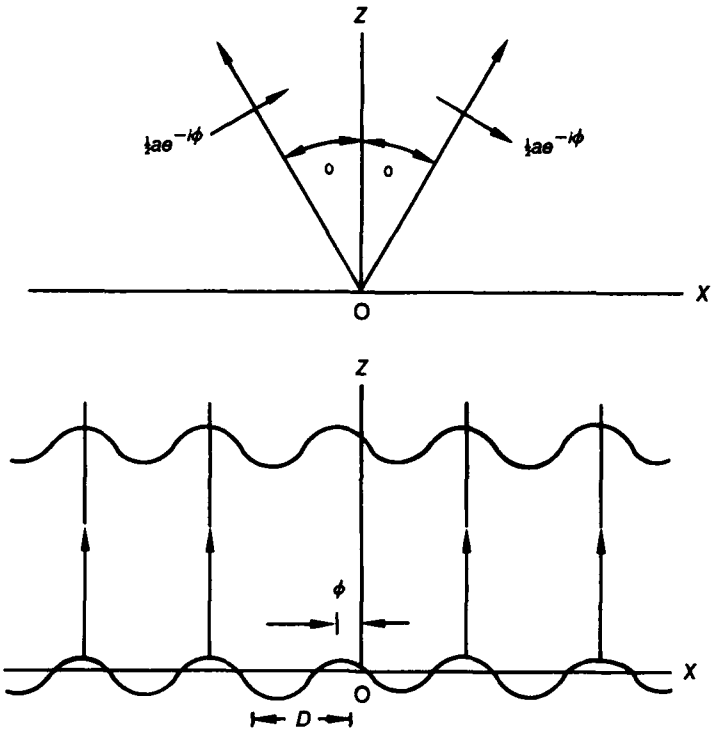

Figure 2. Illustrating the angular spectrum and resulting waveform for a two-component system (after Ratcliffe, 1956).

$$v_0 = \frac{v}{(1 - 1/d^2)^{1/2}}$$

The velocity of such a wave is greater than that of the uniform plane wave and depends on the spatial period. For large d (small S_0), the velocity differs only slightly. However, for small d (large S_0), the velocity of the striated wave can differ significantly from the uniform wave.

On the plane $Z = 0$, we have

$$w(x) = a \cos (2\pi S_0 x + \phi)$$

This field could have been produced by allowing a uniform plane wave travelling along $0Z$ to pass through a thin screen which imparts this amplitude on it. The resulting disturbance would be the same as that produced by our two plane waves at θ_0 and $-\theta_0$. They thus represent the angular spectrum corresponding to diffraction by such a screen.

The power of this representation lies in the fact that any function, regular or random, can be synthesized from an angular spectrum of plane waves. Thus the technique, described here for a regular function, can be used for a randomly varying screen, and most of the results we derive here are equally true for that more general case.

Consider now a thin diffracting screen situated in the $Z = 0$ plane which alters the phase of the incident wave without altering its amplitude. This approximation is valid for F-region scintillation modeling when the frequency of the transmitted wave is much larger

than the ion-electron collision frequency. We suppose that as the wave emerges from such a screen, the phase varies along the X direction according to

$$\phi(x) = <\Delta\phi^2>^{1/2} \cos(2\pi x/d)$$

where $<\Delta\phi^2>^{1/2}$ is the rms value of the phase deviation imparted by the screen. When an "equivalent" screen is used to replace an extended propagation region, such as the F-region of the ionosphere, $<\Delta\phi^2>^{1/2}$ represents the rms value of the phase fluctuations measured at a receiver after the wave has traversed the medium.

For a normally incident uniform plane wave of unit amplitude, the field at $Z = 0$ is

$$w(x) = e^{[i<\Delta\phi^2>^{1/2}\cos(2\pi x/d)]} \tag{5}$$

In order to determine the angular spectrum corresponding to Eq. 5, we use the familiar expansion, with $\eta = 2\pi x/d$ (Gradshteyn, Ryzhik, 1965):

$$e^{[i<\Delta\phi^2>^{1/2}\cos(\eta)]} = \sum_{n=-\infty}^{\infty} (i^n) J_n(<\Delta\phi^2>^{1/2})\, e^{in\eta}$$

where J is the cylindrical Bessel function of the first kind.

Thus

$$w(x) = \sum_{n=-\infty}^{\infty} (i^n) J_n[<\Delta\phi^2>^{1/2}]\, e^{in\eta}$$

We showed above that $w(x)$ and $W(S)$ are Fourier transform pairs, and so we can write Eq. 2 as

$$w(x) = \sum_{n=-\infty}^{\infty} W(S_n)\, e^{i2\pi S_n x}$$

Comparing these two expressions for $w(x)$, we see that the spectrum $W(S)$ has components at values $S = 0, 1/d, -1/d, 2/d, -2/d, \ldots, n/d, -n/d \ldots$. The amplitude of the side components is $i^n J_n(<\Delta\phi^2>^{1/2})$ and changes by $\pi/2$ between successive components. However, $J_n(<\Delta\phi^2>^{1/2})$ is small for $n > <\Delta\phi^2>^{1/2}$ and so there is little energy in those components for which $S > <\Delta\phi^2>^{1/2}/d$.

For $<\Delta\phi^2>^{1/2} < 1$ radian, the angular spectrum for the sinusoidal phase screen extends to components at $1/d$ and $-1/d$. The amplitudes of the side components are in quadrature with the main component at $S = 0$. If $<\Delta\phi^2>^{1/2} > 1$ radian, the so-called "deeply modulated" phase screen, the angular spectrum extends to components at approximately + and $-<\Delta\phi^2>^{1/2}/d$. Each component amplitude increases $\pi/2$ in phase relative to the undeviated component at $S = 0$. In particular, the largest angle component at $S \sim <\Delta\phi^2>^{1/2}/d$ differs in phase with respect to the $S = 0$ component by $<\Delta\phi^2>^{1/2}\pi/2$. The angular spectrum here depends jointly on the spatial period and the depth of the modulation $<\Delta\phi^2>^{1/2}$.

We have established the relationship between the field distribution at the diffracting screen and the angular spectrum. Now we want to determine the field distribution at planes separated from the phase screen. In particular, at a plane located at some $z = z'$ where $z' \gg 1$.

Again we consider a uniform, unit amplitude plane wave normally incident on a one-dimensional phase-changing screen at $Z = 0$. The wave passes through the screen, and the field amplitude at any point x,z is given by Eq. 4. As the striated wave formed by spectral components in direction $\pm S$ propagates from a point $x,0$ to a point x,z', its phase, β, changes by $2\pi(Sx + Cz') - 2\pi Sx$ or, with $C = (1 - S^2)^{1/2}$ and $S \ll 1$

$$\Delta\beta = 2\pi z' - \pi S^2 z'$$

The first part of this equation represents the phase change of the direct ($S = 0$) component in travelling to the $z = z'$ plane. The second part represents the phase gain by the striated wave. If $g(x)$ represents the complex field amplitude on the plane at $z = z'$ with phase referenced to the point x,z', then $g(x)$ is synthesized from the same angular spectrum as that which makes up $w(x)$ on the phase screen at $z = 0$. However, each component wave is advanced in phase by $\pi z' S^2$. This is entirely equivalent to the usual Huygen-Fresnel method of determining the diffraction field via equivalent current sources and Greens function (Ratcliffe, 1956).

As an example of the above analysis, we apply it to the sinusoidal phase screen. Let the field at the screen be given by Eq. 5. If $\langle\Delta\phi^2\rangle^{1/2} < 1$ radian, we can expand to first order to obtain

$$w(x) = 1 + i\langle\Delta\phi^2\rangle^{1/2} \cos(2\pi x/d)$$

or, equivalently

$$w(x) = 1 + \frac{i\langle\Delta\phi^2\rangle^{1/2}}{2} (e^{i2\pi Sx} + e^{-i2\pi Sx})$$

where we have let $S = 1/d$. Thus, the spectrum contains components at $S = 0$, $1/d$, and $-1/d$, as we indicated earlier.

It was shown earlier that the striated wave formed by the two side components travels at a greater velocity than the plane wave. At a certain distance, the striated wave, which is in quadrature with the main wave at the screen, will advance in phase with respect to the main wave and will be in phase or antiphase with it. At this distance, the two waves will combine to produce amplitude variations in the total field. From above, this occurs at the plane $z = z'$ where $\pi S^2 z' = \pi/2$ or $z' = d^2/2$. The field distribution at this plane is given by

$$g(x) = 1 - \langle\Delta\phi^2\rangle^{1/2} \cos(2\pi x/d)$$

Thus, the period of the amplitude variation is the same as that of the phase variation in the screen.

As the waves continue to advance in the Z direction, the striated wave gains $\pi/2$ radians in phase on the main wave at each distance increment of $d^2/2$. When they are in phase or antiphase, they combine to produce amplitude variations, and they produce phase variations when they are in quadrature.

These results show that when the phase fluctuations are weak ($\langle\Delta\phi^2\rangle^{1/2} < 1$), amplitude fluctuations first develop on a plane at distance Z' from the diffracting screen, for which $F = D$. Here D is the spatial period of the phase variations at the screen and $F = \sqrt{2\lambda Z'}$ is the Fresnel zone size on the screen at a distance Z'. The amplitude fluctuations have the same spatial size as the phase variations in the screen.

Next we consider a sinusoidal phase screen for which $<\Delta\phi^2>^{1/2} >> 1$ radian. Here, the angular spectrum extends to components for which $|S| \sim n/d$, where $n \sim <\Delta\phi^2>^{1/2}$. Each of these side components is advanced by $\pi/2$ radians in phase on its predecessor and by $n\pi/2$ on the main wave ($S = 0$). If we examine the field at a series of planes at increasing distances from the diffracting screen, the striated waves formed by component pairs will "catch up" with the main wave at certain distances. The component in the direction nS will gain $\pi/2$ radians in phase on the main wave when it has travelled a distance $\pi z n^2 S^2 = n\pi/2$ or $z = (2nS^2)^{-1}$. At this distance, the component wave will combine with the main wave to produce an amplitude modulation with a spatial period of $1/nS$ or d/n. As the wave advances, each successive component wave will combine with the main wave to produce a different amplitude modulation wavelength. The higher order component waves, corresponding to smaller spatial components, travel fastest and are the first to produce amplitude modulation at planes closest to the diffracting screen. Thus, at all distances, the diffraction field contains spatial periods smaller than the spatial period of the screen itself.

To see these effects more quantitatively, consider the largest order component wave for which $S \sim <\Delta\phi^2>^{1/2}/d$. This component wave produces its effect on the amplitude fluctuations on a plane at z' determined by $\pi z'(<\Delta\phi^2>^{1/2}/d)^2 = <\Delta\phi^2>^{1/2} \pi/2$ or for z' given by $z' = d^2/2<\Delta\phi^2>^{1/2}$. In terms of the Fresnel zone size F, this becomes

$$F = D/<\Delta\phi^2>^{1/4} \tag{6}$$

We then have amplitude variations developed on planes for which the Fresnel zone is smaller than the spatial period of the phase screen. This is in contrast to the results for $<\Delta\phi^2>^{1/2} < 1$, where we found amplitude variations first develop in a plane for which $F = D$. The large phase fluctuations here are causing the screen to act as an optical lens to produce focusing in a plane closer to the screen.

The spatial period, call it l, of the amplitude variations produced on the plane at z' is $d/<\Delta\phi^2>^{1/2}$. Then with $l = L/\lambda$, we have

$$L = D/<\Delta\phi^2>^{1/2} \tag{7}$$

and we see that the smallest period amplitude fluctuations are less than the spatial period of the phase screen. Again, this is to be contrasted to $<\Delta\phi^2>^{1/2} < 1$, where we found the spatial period of the amplitude variation is D.

Now consider a sinusoidal phase screen at $Z = 0$ and a reception plane at some distance Z for which the Fresnel zone size is F. Let $<\Delta\phi^2>^{1/2} >> 1$ and $D >> F$. For these conditions, we are concerned with the lens-like refractive scattering (Booker, MajidiAhi, 1981) described above. Such a screen will produce foci in a plane parallel to the screen. These foci lie in the reception plane at Z if, from Eq. 6

$$D = F<\Delta\phi^2>^{1/4} \tag{8}$$

Thus, to focus a sinusoidal phase screen of wavelength D at a reception plane specified by F requires that

$$<\Delta\phi^2> = (D/F)^4 \tag{9}$$

In such a focal plane, the wavelength D can be determined, since it represents the distance between focal spots. The focal spot size is given by Eq. 7. Thus, for a given screen wavelength, the larger the rms plane fluctuations, the closer the focal plane to the screen and, also, the sharper the focal spot size.

The fine structure in the reception plane is associated with the arrival at the plane of angular spectrum components which are approximately co-phased within a cone angle of $\pm\lambda/L$. This, in turn, is controlled by the distance across the phase screen over which the field has approximately uniform phase, a distance given by Eq. 7. So for refractive scattering, fine structure in any reception plane is the same as it is in the focal plane. However, in planes displaced from the focal plane, the amplitude variation no longer has the form of an array of focal spots of width L and separation D. Out of the focal plane, interference by other component waves with slightly different phase causes an amplitude variation with fine structure L superimposed on a gross modulation of wavelength D (Booker, MajidiAhi, 1981).

In summary, we see that one can describe the effects of a sinusoidal phase-changing screen in terms of the sizes of the amplitude variation structure which it produces on displaced planes. When $<\Delta\phi^2>^{1/2} < 1$, amplitude variations are produced at distant planes for which the Fresnel zone size is equal to the wavelength in the screen. The amplitude variations have a characteristic size approximately equal to the wavelength in the screen. This is commonly referred to as weak or single scattering and, for the ionosphere, is generally the situation for very high frequencies or very quiescent conditions.

In contrast to the weak scattering situation, we have the strong or refractive scattering condition for which $<\Delta\phi^2>^{1/2} >> 1$ radian. For strong scattering, higher order components in the angular spectrum produce fine amplitude variation structure ($<D$). The fine structure is produced on planes closer to the phase screen.

These results now need to be generalized to the more complicated irregular phase screen. As we indicated earlier, the irregular structure of the ionosphere is characterized by a random distribution of irregularities covering a large range of scale sizes. In order to use the phase-changing-screen modeling technique, we must relate the observed irregular structure of the density irregularities to the properties of the phase screen. To do this, we will relate the power spectrum of the phase variations produced by the screen to the power spectrum of the irregularities.

Consistent with the above discussion, we consider a wave which is normally incident on a plane ionospheric layer of thickness ΔL. We assume the background electron density is a function of the vertical coordinate z only, where x,y,z now have the usual units of distance. Within the plasma layer, there exist electron density irregularities describable by a three-dimensional power spectrum, $S_N(k_x,k_y,k_z)$. If we consider only that part of the spectrum for which the irregularities are much larger than the wavelength, we may apply geometric optics. Under this approximation, the phase at a point x,y in a plane at z, $z > \Delta L$, is given by

$$\phi(x,y) = k \int_0^{\Delta L} n(x,y,z)dz \tag{10}$$

where n is the index of refraction within the layer. The variation in the phase observed at the point x,y due to variation in the index of refraction along the ray is

$$\Delta\phi\,(x,y) = k \int_0^{\Delta L} \Delta n(x,y,z)dz \tag{11}$$

Note that in Eq. 11, we are calculating the phase variation due to spatial variation in the index of refraction along a deterministic ray. Under very strong scattering conditions, there may be many rays reaching the point x,y. In those conditions, Eq. 11 represents the phase variation along a "representative" ray.

If we do a similar calculation for a ray which reaches a point $x + \Delta x$, $y + \Delta y$ and form the averaged product with Eq. 11, we have

$$<\Delta\phi(x,y)\Delta\phi(x + \Delta x, y + \Delta y)>$$

$$= k^2 \int_0^{\Delta L} \int_0^{\Delta L} <\Delta n(x,y,z)\Delta n(x + \Delta x, y + \Delta y, z')>dzdz' \tag{12}$$

where we assume Δn is a random function of position and brackets represent the ensemble average, i.e., average over all possible configurations of the random function at a given point.

The index of refraction in the ionosphere is actually a function of space and time; however, in Eq. 11 and 12, we have ignored this temporal dependence. The assumption is that during the time that a wave takes to traverse the distance ΔL, the ionosphere is approximately constant, except for bulk drift motion. This assumption of a frozen ionosphere simplifies the calculations.

To proceed, we require a model for the variation in index of refraction appearing in Eq. 12. For HF and higher frequencies, we will ignore the propagation effects of the earth's magnetic field and the damping effects of electron-ion and electron-neutral collisions. The ionosphere is then describable by the cold plasma dispersion relation

$$n = (1 - e^2 N/\epsilon_0 m\omega^2)^{1/2} \tag{13}$$

where e and m are the charge and mass of the electron, respectively, ϵ_0 is the free-space permittivity, and $\omega = 2\pi f$ is the operational angular frequency. $N(z)$ is the height-dependent electron density.

For our purposes of relating the spatial properties of the irregularities to those of the phase spectrum, we will assume $\omega^2 >> e^2 N/\epsilon_0\, m$ and so, to first order in ΔN, we have from Eq. 13

$$\Delta n \sim \frac{e^2 \Delta N}{2\epsilon_0 m\omega^2}$$

Assuming ΔN is a zero mean, homogeneous, random function of position, Eq. 12 becomes

$$\rho_\phi(\Delta x, \Delta y) \propto \int_0^{\Delta L} \int_0^{\Delta L} \rho_N(\Delta x, \Delta y, z - z')\, dzdz' \tag{14}$$

where ρ_ϕ, ρ_N are the autocorrelation function of phase and electron density, respectively. In Eq. 14, the homogeneity of ΔN has allowed us to write the autocorrelation as a function of the difference in coordinates between the two points (Panchev, 1971).

The integral in Eq. 14 is simplified by a change to the variables $\alpha = z - z'$, $\beta = (z + z')/2$. Then, for a layer thickness much larger than the outer scale of irregularities, Eq. 14 becomes

$$\rho_\phi (\Delta x, \Delta y) \propto \int_{-\infty}^{\infty} \rho_N(\Delta x, \Delta y, \alpha) d\alpha \tag{15}$$

The integration limits have been extended to $\pm\infty$ in Eq. 15 since $\rho_N = 0$ for α greater than the vertical outer scale size. This equation relates the two-dimensional spatial autocorrelation function of phase to that of the irregularities within the layer. The horizontal power spectrum is obtained from Eq. 15 by Fourier transformation in horizontal coordinates (Panchev, 1971; Tatarskii, 1971).

For a three-dimensional autocorrelation function of irregularities, the power spectrum S_N is given by

$$S_N (k_x, k_y, k_z) = \int_{-\infty}^{\infty} \int \int \rho_N(\Delta x, \Delta y, \Delta z)\, e^{i\bar{k}\cdot\Delta\bar{r}}\, d(\Delta\bar{r})$$

where $\Delta\bar{r} = (\Delta x, \Delta y, \Delta z)$.

A two-dimensional spectrum in the plane at z is then given by

$$F_N (k_x, k_y, \Delta z) = \int_{-\infty}^{\infty} \int \rho_N(\Delta x, \Delta y, \Delta z)\, e^{i(k_x \Delta x + k_y \Delta y)} d(\Delta x) d(\Delta y)$$

From these two expressions, we see that

$$S_N (k_x, k_y, k_z) = \int_{-\infty}^{\infty} F_N (k_x, k_y, \Delta_z)\, e^{ik_z \Delta z} d(\Delta z)$$

So, if we perform a two-dimensional Fourier transform of Eq. 15 with respect to Δx, Δy, we find

$$\phi(k_x, k_y) \propto S_N (k_x, k_y, 0) \tag{16}$$

Thus, the two-dimensional power spectrum of phase in the plane at z is simply related to the three-dimensional spectrum of irregularities. In particular, for a power law irregularity spectrum, the phase spectrum is also of power law form. Integration of Eq. 16 along y shows that, similarly, the one-dimensional phase spectrum is proportional to the two-dimensional irregularity spectrum.

Uscinski *et al.* (1981) have treated a one-dimensional phase screen with a power law spectrum of phase fluctuations with spectral index 4. This corresponds to a two-dimensional screen with spectral index 5. When the rms phase fluctuations are large compared to 1 radian and the outer scale of irregularities, L_o, is large compared with the Fresnel scale, Uscinski *et al.* find that the fine scale structure in the intensity variation pattern is given approximately by

$$I = \frac{L_o}{\langle \Delta\phi^2 \rangle^{1/2}} \tag{17}$$

Comparison with Eq. 7 shows that in going from a one-dimensional sinusoidal phase screen to an irregular power law screen with spectral index 4, the fine structure, or focal scale, is determined by replacing the sinusoidal wavelength by the outer scale of irregularities (Booker, MajidiAhi, 1981).

Booker and Tao (1987) have shown that for a one-dimensional phase screen with spectral index $1 < p < 3$, Eq. 17 must be modified to

$$l = \alpha \frac{L_o}{<\Delta\phi^2>^{1/(p-1)}} \tag{18}$$

where α is a numerical coefficient which is a function of p. Similar results apply to a two-dimensional screen with a spectral index $p + 1$.

In Fig. 3, several examples of intensity power spectra are shown. These data were derived from the signal of the ATS-6 beacon satellite at Boulder, Colorado, in January 1975. Simultaneous data at three frequencies are shown in the figure. At the two higher frequencies, the S_4 index, which is the normalized variation of the intensity about the mean, is less than 1. This is representative of weak-to-moderate scattering. At 40 Mhz, however, the S_4 index is greater than 1, indicative of a strong, multiple-scatter condition, as described above. Note that the spectra in this case extend to high normalized frequencies, corresponding to the fine scale structure produced under these conditions.

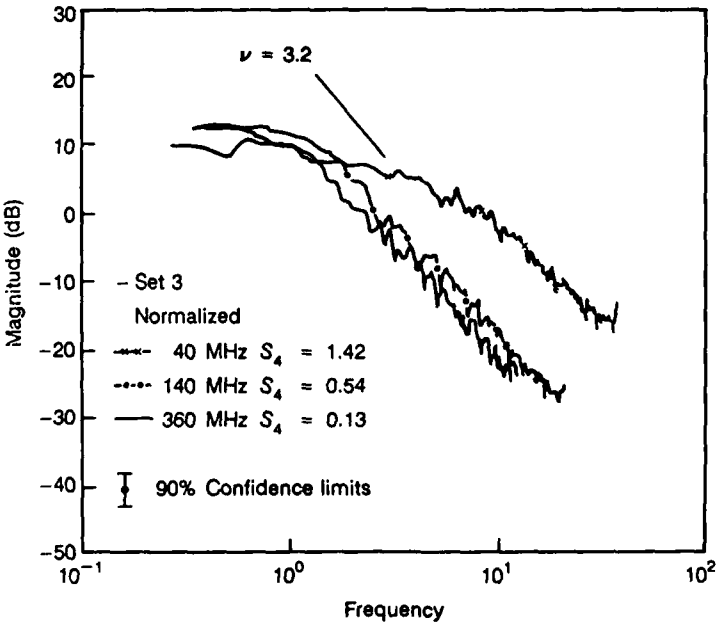

Figure 3. Illustrating intensity power spectra for 40, 140, and 360-MHz signals transmitted from the beacon satellite ATS-6. The 140 and 360-MHz spectra are indicative of weak scattering, while the 40-MHz spectrum is typical of strong scattering. (After Umeki, *et al.*, 1977.)

Using the theory outlined above for the deeply modulated phase screen, Booker and MajidiAhi (1981) have generated the intensity spectra shown in Fig. 4. They assumed a power law phase spectrum with a spectral index $p = 3$, an outer scale $l_o = 10\ F$, and an inner scale $L_i = 10^{-2}\ F$, where F is the Fresnel scale. Various values of the mean square phase fluctuation were used in Fig. 4 to produce the multiple plots.

Referring to Fig. 4, we see that for $\langle\Delta\phi^2\rangle \leq 10$ radians, the scatter is weak and the normalized spectra show a single peak at approximately the Fresnel scale. As $\langle\Delta\phi^2\rangle$ is allowed to increase, the small scale structure begins to emerge and the spectra extend to higher frequencies. In this instance, the focal scale, l, as defined above and indicated by the x in Fig. 4, corresponds approximately to the high-frequency roll-off point in the spectrum. Note in Fig. 4 that the lens scale is also indicated on the plots. Comparison to Fig. 3 shows that, qualitatively, the predicted spectra are similar to those seen under strong multiple-scatter conditions.

So far, we have indicated that the rms phase fluctuation must be larger than 1 radian for multiple refractive scattering to dominate weak diffractive scattering. However, in Fig. 4, weak scatter dominates even for rms phase fluctuations greater than 3 radians. We want now to determine approximately how large the phase fluctuation must be for the small scale structure given by Eq. 18 to develop.

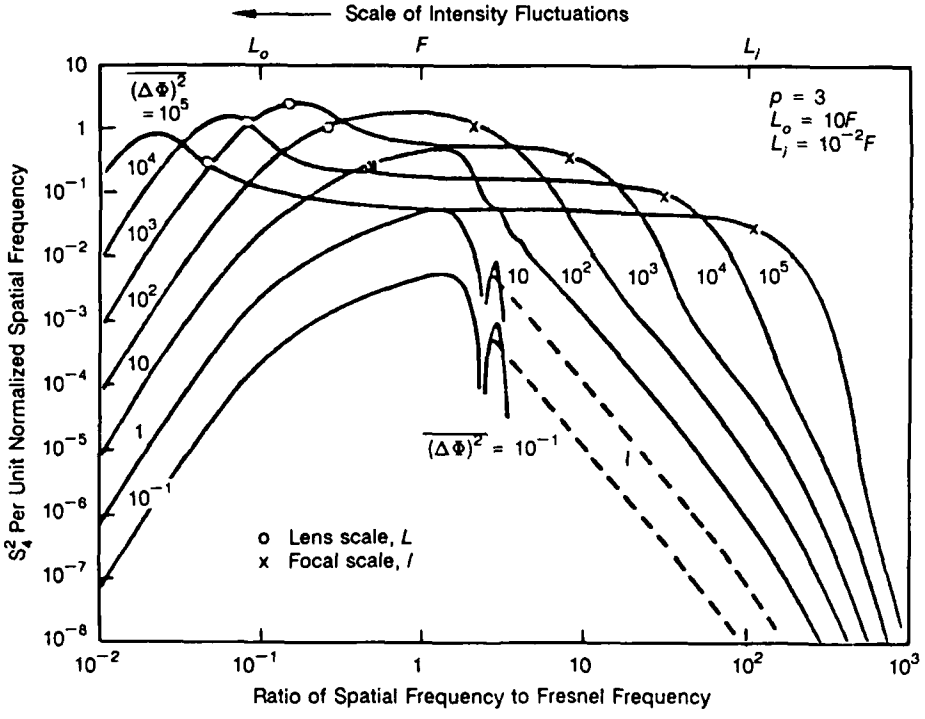

Figure 4. Intensity power spectra generated by using the multiple refractive scatter model. Calculations utilized a $p = 3$ power law phase spectrum with an outer scale $L_o = 10F$ and an inner scale $L_i = 10^{-2}F$, where F is the Fresnel scale. Curves shown are parameterized by the mean square phase fluctuations. (After Booker, MajidiAhi, 1981.)

Consider, then, a random plasma slab containing irregularities of electron density describable by a power law spectrum between some outer scale L_o and inner scale L_i . Also assume that a reception plane parallel to the slab lies at some distance z. For most ionospheric scintillation phenomena, $L_o >> F$, where F is the Fresnel scale for the plane at z. In fact, this is a requirement for the validity of the multiple refractive scatter theory.

We wish to model this situation with an equivalent phase-changing screen which will replace the actual scattering medium. Under conditions of multiple refractive scattering, there are multiple rays joining a transmitter to a receiver in the reception plane. This is illustrated schematically in Fig. 5a, with the equivalent phase screen depicted in Fig. 5b. Associated with each of these rays is a Fresnel zone of scale F. These zones are distributed across the phase screen with a scale L, which we have called the lens scale, given here by

$$L = F^2/l \tag{19}$$

where l is the focal scale.

In order for there to be many Fresnel zones across the screen, we must have

$$L >> F$$

or, from Eq. 19

$$l << F \tag{20}$$

From Eq. 18, then, for a one-dimensional screen with spectral index $1 < p < 3$ or a two-dimensional screen with spectral index $2 < p < 4$, multiple refractive scattering dominates diffractive scattering when

$$<\Delta\phi^2> >> \left(\frac{\alpha L_o}{F}\right)^{p-1} \tag{21}$$

Since $L_o >> F$ and $p > 1$, $<\Delta\phi^2>$ must be very large for the simple theory outlined above to hold, or equivalently, the wavefront must be scattered many times.

Now the focal scale, l, is associated with the arrival at the reception of rays spread over a cone of half-angle $\lambda/2\pi l$. This angle, in most cases, is small compared with 1 radian. Under severe scattering conditions, however, the accumulated scattering angle may approach 1 radian. Under such conditions, the correlation scale in the reception plane approaches $\lambda/2\pi$ and the ionosphere is acting as a diffuse scatterer. This is the minimum correlation scale observed (Booker, Tao, 1987).

To summarize, the correlation structure of the intensity variation varies according to Eq. 18. When l, calculated according to Eq. 18, is greater than the Fresnel scale F, the scattering is weak and intensity variations of scale, F, are observed at the reception plane. When l is less than F but greater than $\lambda/2\pi$, multiple refractive scattering is dominating single diffractive scattering and the intensity correlation scale is given by l. When $l < \lambda/2\pi$, the ionosphere has become a diffuse scatterer, with incoming radiation spread over a cone half-angle of approximately 1 radian. In this case, the correlation scale l is about $\lambda/2\pi$.

Using the multiple refractive scale theory, it is possible to determine several other properties of the scattered wave which are useful in many applications. These include the correlation bandwidth (Booker, Tao, 1987), the larger scale intensity variation at the lens

scale, L, which Booker called "twinkling" (Booker, Tao, 1987), and the half-angle of the cone over which radiation arrives at the reception plane under various scattering conditions. For our purpose in this report, we will not deal directly with these quantities. The interested reader is referred to the Reference section for more information (Booker, 1979; Booker, Tao, 1987).

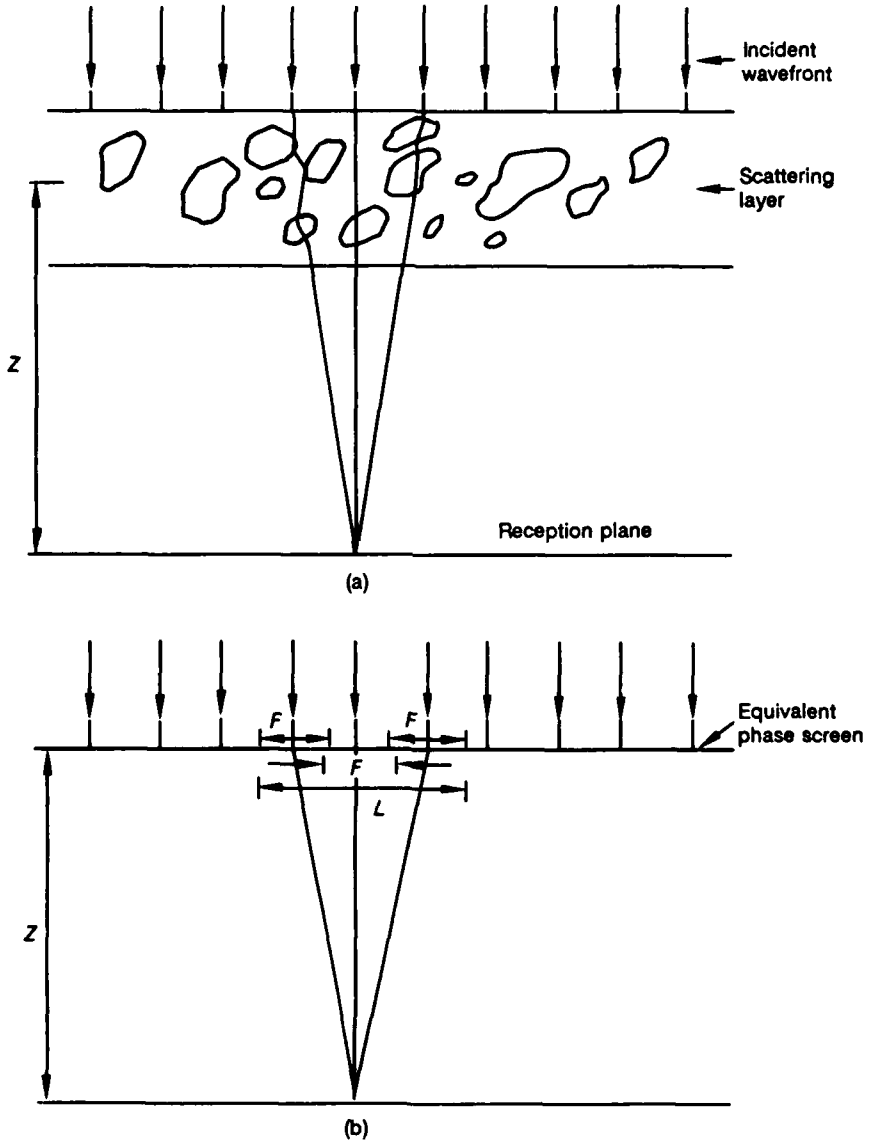

Figure 5. Schematic of the phase-screen modeling method. In (b), the relationship between the lens scale, L, and the Fresnel scale, F, is shown for a strong scattering condition.

IMPLEMENTATION OF THE MULTIPLE REFRACTIVE SCATTER MODEL

A typical operational scenario is depicted in Fig. 6. In this figure, a satellite in earth orbit transmits a signal at low VHF or HF which is received at one or more earth-based locations. We wish to determine the phase correlation of the signal at points separated in the reception plane by a lag $\Delta\bar{r}_0$.

As we showed earlier, the two-dimension phase power spectrum $\phi(\bar{k})$ in a plane parallel to the equivalent phase screen is simply related to the three-dimension power spectrum of electron density irregularities $S_N(\bar{k},k_z)$ by the relation

$$\phi(\bar{k}) \propto S_N(\bar{k},k_z = 0)$$

where, referring to Fig. 6, $\bar{k} = k_x\,\hat{x} + k_y\hat{y}$. In our current version of the model, we assume that the electron density irregularities are three-dimensionally isotropic with a power law spectrum for irregularities smaller than the outer scale, L_o . We take the inner scale to be zero.

We assume initially that the spectrum is adequately described by a single spectral index, p. However, as we indicated earlier, there is some evidence that a two-spectral-index model may be necessary in some situations. Following Booker and Tao (1987), who assumed a one-dimensional spectrum with spectral index of 2.4, we take p to have the value 3.4.

Thus, we write the phase power spectrum in a plane parallel to the phase screen as

$$\phi(k_x,k_y) = <\Delta\phi^2>^{1/2}\, S(k_x,k_y) \tag{22}$$

where

$$S(k_x,k_y)\ \alpha\ \frac{1}{[1 + (k_x^2 + k_y^2)L_o^2]^{p/2}}$$

$<\Delta\phi^2>$ is the mean square fluctuation of phase and L_o is the outer scale at the height of the phase screen.

Since

$$\frac{1}{(2\pi)^2}\int_{-\infty}^{\infty} \phi(\bar{k})d\bar{k} = <\Delta\phi^2>$$

we must have

$$\frac{1}{(2\pi)^2}\int_{\infty}^{+\infty} S(\bar{k})\, d\bar{k} = 1$$

So, normalizing $S(\bar{k})$, we find

$$S(k_x,k_y) = \frac{4\pi L_o^2\,\Gamma(p/2)}{\Gamma(p/2 - 1)}\ \frac{1}{[1 + k^2L_o^2]^{p/2}} \tag{23}$$

where Γ is the gamma function and $k^2 = k_x^2 + k_y^2$.

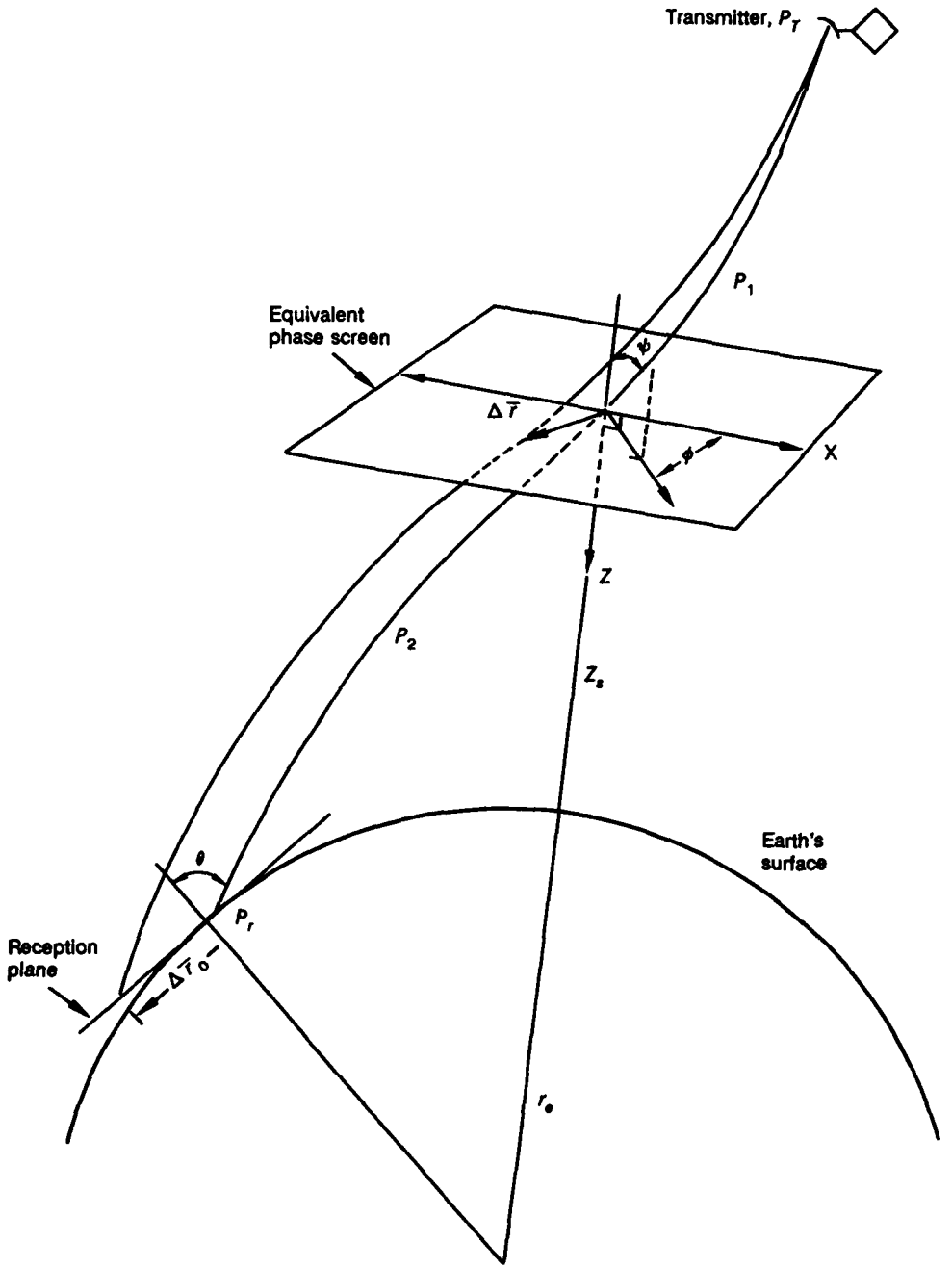

Figure 6. Schematic of a typical operational scenario. Indicated is the geometrical relationship between the phase screen and the transmitter and receiver. P_1 and P_2 are group paths along the indicated portions of the ray, θ is the zenith angle of the ray at the reception plane, ψ and ϕ are the zenith and azimuthal angles at the phase screen, respectively.

The two-dimensional phase autocorrelation function in a plane parallel to the screen is given by the Fourier transformation of the power spectrum. So

$$<\Delta\phi^2> \rho_\phi (\Delta\bar{r}) = \frac{1}{(2\pi)^2} \int_{-\infty}^{\infty} \int_{-\infty}^{\infty} e^{i\bar{k}\cdot\bar{r}} \phi(\bar{k}) d\bar{k} \tag{24}$$

when $\Delta\bar{r} = \Delta x\hat{x} + \Delta y\hat{y}$. As we indicated earlier, we are assuming the fluctuation of electron density is describable as a homogeneous random function. In that case, the phase autocorrelation is a function of the difference in coordinates only.

Combining Eq. 22, 23, and 24, we find

$$\rho_\phi(\Delta r) = \frac{2}{\Gamma(p/2 - 1)} (\Delta r/2L_o)^{\frac{p-1}{2}} \quad K_{\frac{p-1}{2}} (\Delta r/L_o) \tag{25}$$

where $\Delta r^2 = \Delta x^2 + \Delta y^2$ and K_v is the modified Bessel function of the second kind.

Referring to Fig. 6, we see that, in general, the reception plane is not parallel to the phase screen. Therefore, we must express the lag $\Delta\bar{r}_0$ in the (x,y,z) coordinate system of the phase screen. Let $\Delta\bar{r}_0$ have components $(\Delta x,\Delta y,\Delta z)$ in the (x,y,z) coordinate system. Then, assuming the rays are approxi ~ately straight in the region near the phase screen, we have

$$\Delta x_s \approx \Delta x - \tan\psi \cos\phi \, \Delta z$$

$$\Delta y_s \approx \Delta y - \tan\psi \sin\phi \, \Delta z$$

where $(\Delta x_s,\Delta y_s)$ are the components of the equivalent lag in the phase screen. Here, ψ is the zenith angle of the ray connecting the transmitter to the receiver, measured at the phase screen, and ϕ is the azimuth.

Finally, the effective lag must be modified to include the spreading effect due to the finite distance to the point source. Referring to Fig. 6, let P_1 be the group path along the ray connecting the transmitter to the penetration point in the screen and let P_2 be that connecting the screen to the receiver. Then, the effective lag in the screen corresponding to $\Delta\bar{r}_0$ is given by

$$\frac{P_1}{P_1 + P_2} |\Delta\bar{r}_s| \tag{26}$$

where

$$|\Delta\bar{r}_s| = (\Delta x_s^2 + \Delta y_s^2)^{1/2}$$

Perhaps the most important parameter for determining the nature of the scattering for transionospheric propagation is the mean square phase fluctuation, $<\Delta\phi^2>$. As we pointed out earlier, phase fluctuations build up as a wave propagates through an extended medium. A single receiver also measures increased phase fluctuations as the time interval over which phase measurements are made is increased. This is due to the effective drift motion of the ionosphere, which brings larger scale irregularities into play as the measurement time is increased. Phase fluctuations peak when sufficient time has allowed outer-scale irregularities to contribute to these fluctuations. While diffractive scattering by

smaller scale irregularities (~ Fresnel scale) contributes to the total phase fluctuations, most of the content is due to refractive scattering by outer-scale irregularities. This is true even when intensity fluctuations are small.

Consider a wave incident on an isotropic electron density irregularity of scale size L_o . According to geometrical optics, the mean square phase fluctuation due to such an irregularity is

$$\langle \Delta\phi^2 \rangle_0 = k^2 L_o^2 \langle \Delta n^2 \rangle$$

where $\langle \Delta n^2 \rangle$ is the mean square fluctuation of index of refraction associated with the irregularity. Referring to Fig. 6, let Δs be a segment of the ray connecting P_T to P_r where, strictly speaking, $\Delta s \gg L_o$. Then there are approximately $\Delta s / L_o$ irregularities along that ray path segment, and the total mean square phase fluctuations for that segment is

$$\langle \Delta\phi^2 \rangle = \frac{\Delta s}{L_o} \langle \Delta\phi^2 \rangle_0$$

The total mean square phase fluctuation along the ray from P_T to P_r is then

$$\langle \Delta\phi^2 \rangle = k^2 \int_{P_r}^{P_T} L_o(z) \langle \Delta n^2 \rangle \, d\bar{s} \tag{27}$$

where integration is along the deterministic ray connecting P_T to P_r. The outer scale is a function of height and, following Booker and Tao (1987), has the profile shown in Fig. 7. This profile approximates the variation of neutral particle scale height up to approximately 400 km (Booker, Tao, 1987).

In order to calculate $\langle \Delta\phi^2 \rangle$ according to Eq. 27, we must first determine the ray through the background ionosphere which connects P_T to P_r. As before, we assume the background ionosphere is describable by the cold plasma dispersion relation

$$n^2 = 1 - \frac{f_p^2}{f^2} \frac{N(\bar{r})}{N_m} \tag{28}$$

In this form, f_p is the peak plasma frequency and N_m is the peak electron density. In this initial version of the model, we will follow Booker and Tao (1987) and assume that N/N_m is a function of height only. The F-region profile we will use is shown in Fig. 8. This profile is describable by the functional form (Booker, Tao, 1987)

$$\frac{N}{N_m} = \exp\left[\frac{z - z_m}{A} - B \ln\left\{\frac{1 + \exp\left[(z - z_m)/C\right]}{1 + \exp D} + D\right\}\right] \tag{29}$$

where A = 40 log e (km), $B = 3/\log e$, C = 100 km, and $D = \log(C/AB - E)$. We take z_m, the height of the peak electron density, to be 400 km.

The ray connecting P_T to P_r through this ionosphere is found by numerical integration of the spherical coordinate ray equation (Kelso, 1964):

$$\chi = r_e \sin\theta \int_{P_r}^{P_T} \frac{dr}{(n^2 r^4 - r_e^2 r^2 \sin^2\theta)^{1/2}} \tag{30}$$

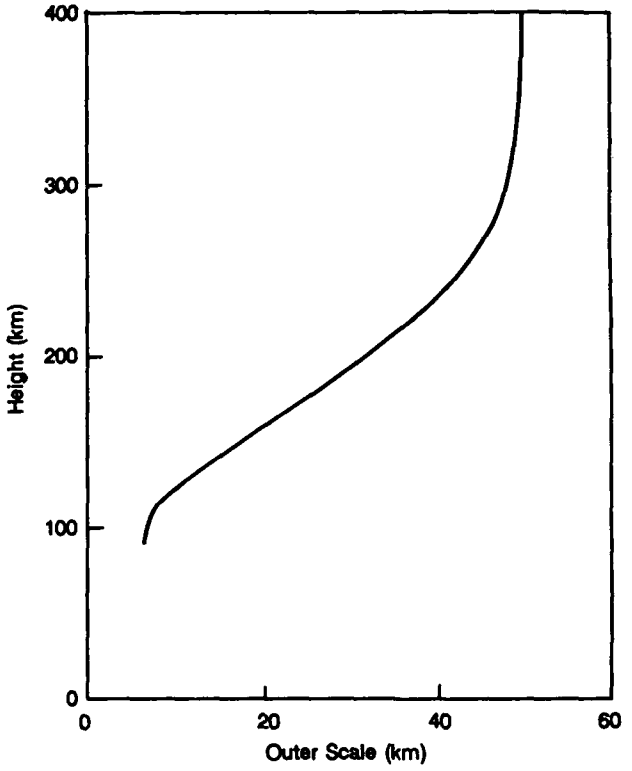

Figure 7. Variation of outer scale with height used in calculation of the mean square phase fluctuations.

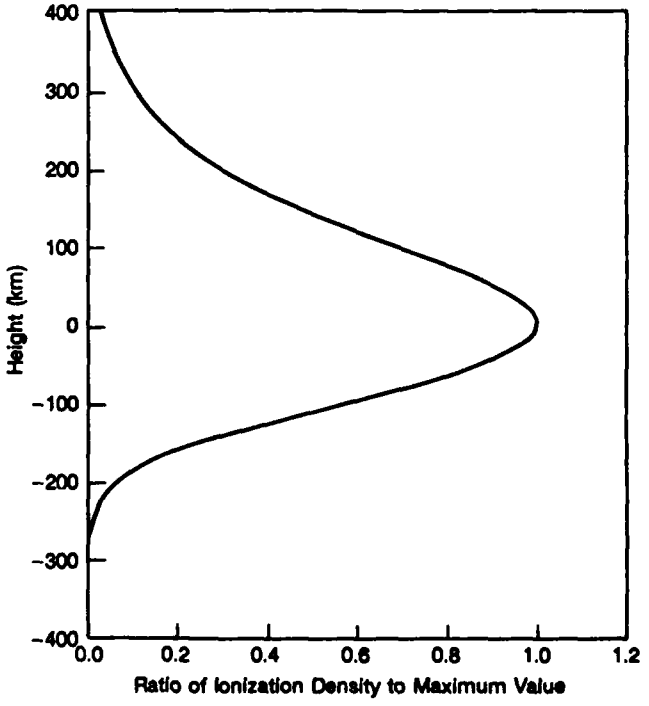

Figure 8. Normalized F-region electron density profile used in the current version of the model.

Here χ is the angle subtended at the center of the earth by the great circle path from the receiver to the subtransmitter point. The radial coordinate is given by $r = r_e + z$, where r_e is the earth's radius and z is height above the earth. The angle θ is the angle of arrival at the earth-based receiver (see Fig. 6). The ray is found by varying the angle θ until the launched ray meets the transmitter.

It remains, in Eq. 27, to determine the mean square fluctuation of index of refraction. Taking differentials in Eq. 28, we have

$$2n\Delta n = -\frac{f_p}{f}\frac{\Delta N}{N_m}$$

Squaring, we have

$$\Delta n^2 = \frac{1}{(2n)^2}\frac{f_p^2}{f^2}\frac{\Delta N^2}{N_m^2}$$

or, taking the ensemble average

$$<\Delta\phi^2> = \frac{(1-n^2)^2}{(2n)^2} < \frac{(\Delta N)^2}{N_m} > \tag{31}$$

The procedure for determining the mean square phase fluctuation is to first determine the ray path through the background ionosphere which connects the transmitter to the receiver. This is done by iteration on θ in Eq. 30. Once this ray is found, we integrate Eq. 27 along that ray.

Another parameter of interest is the mean square fluctuation of the elevation angle θ and azimuthal angle η at the reception plane. For a one-dimensional ionosphere which we are currently using, the rays are confined to vertical planes containing the transmitter and receiver. Thus, we choose that plane as the azimuthal reference plane and so $\eta = 0$ in the following development. However, since our phase screen is two-dimensional, we can calculate the fluctuation in azimuth around zero.

Let $\vec{d}$ be the vector separating two receive antennas located in the reception plane (see Fig. 6). Let d_1 be the component of $\vec{d}$ in the vertical plane containing the receiver and transmitter. We assume $d_1 < L_o$ where L_o is the outer scale of irregularities at the phase screen.

Let ϕ_1/k and ϕ_2/k be the phase path length along the rays connecting the transmitter to the respective receive antennas. Then the elevation angle θ in the reception plane is given approximately by

$$\sin\theta \approx \frac{\phi_1 - \phi_2}{kd_1}$$

For small deviations in θ, we have

$$\Delta(\sin\theta) \approx \Delta\theta = \frac{\Delta\phi_1 - \Delta\phi_2}{kd_1}$$

and so the mean square fluctuation in elevation angle of arrival is approximately

$$<\Delta\theta^2> \approx < \frac{(\Delta\phi_1 - \Delta\phi_2)^2}{k^2 d_1^2} >$$

The phase structure function appearing in the numerator can be expanded and, assuming that the phase autocorrelation function exists and that the statistics of the medium are homogeneous, we find

$$<\Delta\theta^2> \approx \frac{2<\Delta\phi^2>}{k^2 d_1^2} [1 - \rho_\phi(d_1)] \tag{32}$$

where $\rho_\phi(d_1)$ is the phase autocorrelation function. As in our earlier discussion concerning the phase autocorrelation, the effective value of d_1, adjusted for a tilted reception plane and a finite source distance, must be used in Eq. 32. If d_2 is the component of $\vec{d}$ in the direction of increasing azimuth, a similar equation holds for the fluctuations $<\Delta\eta^2>$ in azimuth, with d_2 replacing d_1.

The expression for the mean square phase fluctuation appearing in Eq. 27 refers to the total value of the phase fluctuation. That is, this is the value one would measure if the signals were sampled over a long enough period of time for outer-scale irregularities to contribute to the fluctuations. If the sampling period is less than this, the outer-scale irregularities do not contribute to the measured phase fluctuations and $<\Delta\phi^2>$ is reduced accordingly.

For the measurement of the signal from a geostationary satellite, for example, the largest scale size which contributes to the phase fluctuation is determined by the sampling period and the drift velocity of the irregularities at the height of the phase screen. For a low orbiting satellite, the drift velocity of the irregularities is normally much less than the scan velocity of the line-of-sight between receiver and transmitter. In this case, it is the scan velocity which provides an effective drift velocity at the phase screen. In either case, if the product of the sampling period and effective drift velocity is smaller than the outer scale, the mean square fluctuation of phase is reduced.

However, it is also true that it is not always necessary to sample over a long period to bring all irregularity scales into play. Under conditions of very strong scattering, spread-*F* conditions for example, the lens scale extends over many Fresnel scales. A reasonable sample of various realizations of the irregularity distribution can then be made over a sampling period of only several seconds (Booker, Tao, 1987).

Thus, it is necessary to adjust the mean square fluctuations according to the lens scale, calculated according to Eq. 18 and 19. Booker and Tao (1987) have shown that the effective mean square phase fluctuations are given by

$$<\Delta\phi^2>_{eff} = \begin{cases} [F/L_o]^{p-1} <\Delta\phi^2>, & L < F \\ [L/L_o]^{p-1} <\Delta\phi^2>, & F < L < L_o \\ <\Delta\phi^2>, & L < L_o \end{cases} \tag{33}$$

where $<\Delta\phi^2>$ is given by Eq. 27. It is this value of the mean square phase fluctuation which is to be used in Eq. 32.

This completes the description of the model currently being used for the analysis of angle-of-arrival data. Several aspects need to be improved for the accurate testing of the method. First, a more realistic ionospheric model must be used in conjunction with the irregularity model. It is expected that during the coming year, the Ionospheric Conductivity and Electron Density (ICED) model (Tascione *et al.*, 1987) will be incorporated along with a full three-dimensional ray trace capability. This should greatly improve our ability to accurately determine the ray connecting the transmitter to the receiver.

Further work is also needed to describe the properties of the irregularities. The spatial and spectral properties of irregularities of scale size of several kilometers is fairly well documented and some modeling does exist (Secan, Fremouw, 1983). However, at the lower frequencies of interest here, a major role is played by large scale irregularities. Very little is known about the properties of these irregularities, since their effect has been routinely removed before analysis in previous studies. As we indicated in an earlier section of this report, evidence indicates that the spatial gradient of electron density, ΔN, is approximately proportional to the ambient density, so that $\Delta N/N$ is approximately constant. This assumption is made in our current model and is used in our calculation of the rms phase fluctuations. As crude as this assumption may seem, it reflects current knowledge in the behavior of the irregularity amplitudes.

The three-dimensional structure of the large scale irregularities is also an area in which little is known. Our assumption of isotropic large scale irregularities represents a theoretical "best guess" based on the mechanism for their production.

What will be required to answer these questions is a coordinated experimental effort designed exclusively to investigate the nature of large scale irregularities. Some effort along these lines has already begun,* but a complete global description will require a much greater effort.

SUMMARY

In this report, we have indicated methods for quantitatively determining the effects of strong scatter on locating systems. The theory outlined is relatively simple and, in conjunction with an accurate orbital prediction model, should provide a useful tool for analyzing angle-of-arrival data.

Two things are required to achieve improvement in the accuracy of the method. First, a more realistic description of the background ambient ionosphere is needed for determining the ray connecting the transmitter to the receiver. The accurate determination of this ray will provide an improved estimate of the actual angular location of the transmitter, i.e., the magnitude of the refractive error correction. Also, as we have indicated, the determination of the fluctuation in this angular location caused by scattering from irregularities requires the integration of the irregularity spectrum along this ray. Thus, a more accurate ray determination will result in more accurate estimates of the error in location due to scattering.

---

*S. Basu, Emanuel College, Boston, private communication, 1988.

The requirement for a more accurate deterministic ray determination should be satisfied by the use of the ICED electron density model along with a full three-dimensional ray-tracing capability. This improvement, expected shortly, should greatly increase the accuracy of both aspects of the problem.

The second requirement for improved accuracy is a more realistic model of the irregularity structure. This information is required for the accurate determination of the mean square phase fluctuations which, as shown in this report, is basic for estimating the magnitude of the effect of the scattering. Work along these lines this year is expected to increase the accuracy of the prediction capability of this model.

REFERENCES

Aarons, J., "Global morphology of ionospheric scintillation," Proc. IEEE, **70** (4), 360 (1982).

Booker, H.G., and H.W. Wells, "Scattering of radio waves by the F region of the ionosphere," Terr. Magn. Atmos. Elec., **43**, 249 (1934).

Booker, H.G., J.H. Ratcliffe, and D.H. Shinn, "Diffraction from an irregular screen with applications to ionospheric problems," Phil. Trans. Roy. Soc. A. **242**, 579 (1950).

Booker, H.G., and J.A. Ferguson, "A theoretical model for equatorial ionospheric spread-F echoes in the HF and VHF bands," J. Atmos. Terr. Phys., **40**, 803 (1978).

Booker, H.G., "The role of acoustic gravity waves in the generation of spread-F and ionospheric scintillation," J. Atmos. Terr. Phys., **41**, 501 (1979).

Booker, H.G., and G. MajidiAhi, "Theory of refractive scattering in scintillation phenomena," J. Atmos. Terr. Phys., **43**, 1199 (1981).

Booker, H.G., J.A. Ferguson, and H.O. Vats, "Comparison between the extended medium and the phase-screen scintillation theory," J. Atmos. Terr. Phys., **47**, 381 (1985).

Booker, H.G., and J. Tao, "A scintillation theory of the fading of HF waves returned from the F-region: receiver near transmitter," J. Atmos. Terr. Phys., **49**, 915 (1987).

Clark, D.H., and W.J. Raitt, "The global morphology of irregularities in the topside ionosphere, as measured by the total ion current probe on ERSO-4," Planet Space Sci., **24**, 873 (1976).

Dashen, R., "Path integrals for waves in random media," J. Math. Phys., **20**, 1530 (1979).

Fejer, B.G., and M.C. Kelley, "Ionospheric irregularities," Revs. Geophys. Space Phys., **18**(2), 401 (1980).

Fremouw, E.J., R.L. Leadabrand, R.C. Livingston, M.D. Cousins, C.L. Rino, B.C. Fair, and R.A. Long, "Early results from the DNA Wideband satellite experiment — Complex signal scintillation," Rad. Sci. **13**(1), 167 (1978).

Gradshteyn, I.S., and I.M. Ryzhik, *Tables of Integrals, Series and Products*, New York, Academic Press (1965).

Heelis, R.A., "Electrodynamics and plasma processes in the ionosphere," Rev. of Geophys., **25**(3), 419 (1987).

Hines, C.O., "Internal atmospheric gravity waves at ionospheric heights," Can. J. Phys., **38**, 1441 (1960).

Ishimaru, A., *Wave Propagation and Scattering in Random Media*, Vol. 2, New York, Academia Press (1978).

Kelso, J.M., *Radio Ray Propagation in the Ionosphere*, New York, McGraw Hill (1964).

Livingston, R.L., C.L. Rino, J.P. McClure, and W.B. Hanson, "Spectral characteristics of medium-scale equatorial F-region irregularities," J. Geophys. Res., **86**, A4, 2421 (1981).

McClure, J.P., and W.B. Hanson, "A catalog of ionospheric F-region irregularity behaviour based on Ogo 6 Retarding Potential Analyzer data," J. Geophys, Res., **78**(31), 7431 (1973).

Panchev, S., *Random Functions and Turbulence*, Oxford, Pergamon Press (1971).

Phelps, A.D.R., and R.C. Sagalyn, "Plasma density irregularities in the high-latitude top side ionosphere," J. Geophys. Res., **81** A4, 515, (1976).

Ratcliffe, J.A., "Some aspects of diffraction theory and their application to the ionosphere," Rep. Prog. Phys., **19**, 188 (1956).

Rino, C.L., "A power law phase screen model for ionospheric scintillation," 1. Weak scatter, Rad. Sci., **15**(6), 1135 (1979).

Rino, C.L., and R.C. Livingston, "On the analysis and interpretation of spaced-receiver measurements of transionospheric radio waves," Rad. Sci., **17**(4), 845 (1982).

Rino, C.L., R.C. Livingston, and S.J. Matthews, "Evidence for sheetlike auroral ionospheric irregularities," Geophys. Res. Lett., **5**(12), 1039 (1978).

Secan, J.A., and E.J. Fremouw, "Improvement of the scintillation irregularity model in WBMOD," Defense Nuclear Agency TR-81-241, 28 February 1983.

Singh, M., and E.P. Szuszczewicz, "Composite equatorial spread-F wave number spectra from medium to short wavelengths," J. Geophys. Res., **89**, A4, 2313 (1984).

Tascione, T.P., H.W. Kroehl, and B.A. Housman, "ICED — a new synoptic scale ionospheric model," Proc. Ionospheric Effects Symposium, Springfield, VA, May (1987).

Tatarskii, V.I., *The Effects of the Turbulent Atmosphere on Wave Propagation*, Springfield, VA, U.S. Dept. of Commerce Technical Publication (1971).

Tsunoda, R.J. "High latitude F-region irregularities: A review and synthesis," Defense Nuclear Agency TR-88-44, 15 February 1988.

Umeki, R., C.H. Liu, and K.C. Yeh, "Multifrequency spectra of ionospheric amplitude scintillations," J. Geophys. Res., **82**, 2752, (1977).

Uscinski, B.J., H.G. Booker, and M. Marians, "Intensity fluctuations due to a deep phase screen with a power-law spectrum," Proc. R. Soc. Lond. A., **374**, 503 (1981).

Woodman, R.F., and C. Lahoz, "Radar observations of F-region equatorial irregularities," J. Geophys. Res., **81**, 5447 (1976).

Woodman, R.F., and S. Basu, "Comparison between *in situ* spectral measurements of equatorial F-region irregularities and backscatter at 3m wavelength," Geophys. Res. Lett., **5**, 869 (1978).

Yeh, K.C., H. Soicher, and C.H. Liu, "Observations of equatorial ionospheric bubbles by the radio propagation method," J. Geophys. Res., **84**, 6589 (1979).